

Velocity Pattern Analysis of Multiple Savonius Wind Turbines Arrays

 Open
 Access

 Ahmad Zakaria^{1,*}, Mohd Shahrul Nizam Ibrahim¹
¹ Numerical Simulation Lab, Universiti Kuala Lumpur Malaysia Italy Design Institute, 56100 Kuala Lumpur, Wilayah Persekutuan Kuala Lumpur, Malaysia

ARTICLE INFO

Article history:

 Received 22 January 2020
 Received in revised form 17 March 2020
 Accepted 22 March 2020
 Available online 28 March 2020

Keywords:

CFD analysis; Velocity pattern; Turbine interaction; Wind farm

ABSTRACT

The right location of an individual wind turbine within a wind farm is important in order to gain its optimal power output. Due to the large area involved, an experimental study can be difficult and non-economical. This paper presents a methodology by which the location of downstream turbines can be estimated by using velocity pattern analysis. A wake structure of an isolated helical Savonius turbine with 90° twist angle is first evaluated by a Sliding mesh method incorporating Reynold Average (RANS) turbulence model Spalart Allmaras. The formation of vortices outside the wake is then observed. It was found that by placing a downstream turbine at the location of the strongest vortex occurrence, in this case within the area between 20° to 90° with respect to the advancing blade of the upstream turbine, produces an enhancement of power coefficient to the later. Repeating the same procedure for another downstream turbine also yields the same result. The last turbine of the line array always experiences the highest power coefficient of all. An application of the concept to a 9 turbine array in a V formation reveals an overall power improvement of 11%. However, placing the downstream turbine in other areas of weaker vortex shows insignificant improvement.

Copyright © 2020 PENERBIT AKADEMIA BARU - All rights reserved

1. Introduction

The most important property of a wind turbine is its power coefficient (C_p). It measures the actual power output generated by the turbine. While the horizontal axis wind turbine (HAWTs) enjoys a better power coefficient than their counterpart the vertical axis wind turbines (VAWTs), the former is usually employed at places with a higher wind speed of exceeding 7 m/s. VAWTs are therefore good candidates for low wind speed areas which is the subject of this paper. Typical power coefficient of HAWT is between 0.3 to 0.4 and for VAWT it normally ranges from 0.1 to 0.2. Research has been ongoing to improve this so-called power coefficient ever since.

For single HAWT, this can be achieved via optimal blade geometry [1] or variable pitch blade design [2]. The same procedure can also be applied to the VAWT of Darrieus type [3,4]. However, an

* Corresponding author.

E-mail address: dzakaria@unikl.edu.my (Ahmad Zakaria)

<https://doi.org/10.37934/cfdl.12.3.3138>

augmentation device is needed in order to significantly increase the power coefficient of Savonius type VAWT [5,6]. Another approach to enhance the power coefficient by having multiple wind turbines located at one specific place called a wind farm. The performance of such a wind farm is usually measured by its power density. This is power generated the turbines per unit area. Hence VAWTs have a competitive advantage over HWAT where turbines can be placed in proximity [7]. The overall power coefficient is improved due to the Magnus effect and periodic coupling of the local flow between turbines [8]. The arrangement of the multiple turbines in a specific configuration such as V and I formation based on flying geese had been proven a success with power efficiency increased to 23% [9]. A linear turbine arrangement with an augmentation device is used to achieve a maximum energy yield. The power coefficient is enhanced by 60% [10]. Several configurations of turbine clusters are tested numerically and found that three turbine cluster configuration gives the best overall performance [11]. However, the increase in power output is given in terms of power density.

The algorithms involved in wind farm layout optimization are usually very complex as they involve the integration of the wake model and AI technique such as particle swarm optimization algorithm and GA [9,12]. The power coefficient is enhanced by 20% to 30% for the optimum layout. Turbine relative angle position and gap distance used as the main criteria in enhancing the overall turbine performance [11]. A similar study shows that the overall turbine performance is also affected by the turbine relative phase angle [13]. An efficient turbine configuration was tested for a nine cluster turbines farm and twenty-seven cluster turbines farm. The result shows enhancement in power density for both cases [14]. In the study, the gap distance and turbine relative angle can contribute to space covering for wind farm installation.

However, the challenge is always on how to place these turbines such that that the overall power efficiency is optimal. To understand this phenomenon, it is always good to understand the wake structure of an individual turbine. The area occupied by this wake can be divided into three zones namely low-speed zone, periodic high-speed zone and secondary periodic high-speed zone [9]. Thus the downstream turbines should be placed within the periodic high-speed zone. The present study focuses on the development of a methodology for estimating an optimal multiple helical Savonius turbines layout by velocity pattern analysis. The wake structure of an isolated turbine is first evaluated by the computational fluid dynamics simulation to identify the best location of its downstream turbine. The placement of downstream turbines either on the advancing blade or returning blade of upstream turbines is then studied to examine the velocity pattern interaction between neighboring turbines and its effect on the overall power efficiency. The basic rule established is then applied to other published configurations such as oblique, line array, and V formation. The preliminary results of an ongoing study are presented in this paper.

2. Turbine Configuration

The design specifications for the Savonius turbines are given in Table 1. Figure 1 shows the geometrical parameter of the helical Savonius wind turbine with 90° twist angle.

Table 1
Savonius design specifications

Parameter	Value
Height, H	0.5 m
Diameter, D	0.27 m
Overlap ratio	0.242
Blade thickness	0.003 m
End plate diameter	0.297 m

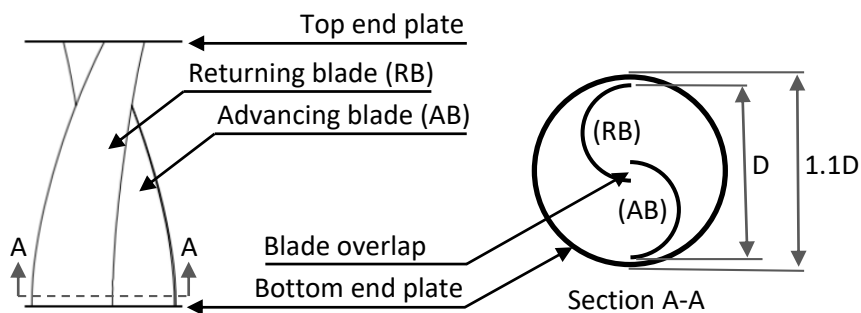


Fig. 1. Geometrical parameter of CFD model

3. Simulation Procedure

The turbine performance evaluation by using CFD is usually involved in several steps. The first step is the development of the computational domain. In this study, a 3D computational domain with a dimension of 30D length x 16D height x 16D width [15] is used. It contains a static domain to represent the environment condition and rotating domain to represent the flow condition around the turbine. The two domains are separated by the interface that provides the continuous interaction of the flow properties between them [16]. The sliding mesh approach is used in order to reduce the computational time since the optimum tip speed ratio is considered in this study [15]. The turbine is placed inside the rotating domain and assigned with specific rotational velocity, ω based on tip speed ratio, TSR relationship as shown in Eq. (1) where R is the turbine radius and V is the wind speed of interest.

$$TSR = \frac{\omega R}{V} \tag{1}$$

The boundary condition is then assigned to the computational domain to demonstrate domain behavior. The boundary condition used in this study is summarized in Table 2. Detailed annotation of boundary conditions can be found in [15].

Table 2
 CFD analysis of boundary condition

Surface name	Boundary condition type	Description
Inlet	Inflow	Inflow velocity type with 5 m/s in x-direction
Outlet	Outflow	Environment pressure
Walls	Slip	-
Blade	Wall	-
Interface	-	-

The accuracy CFD prediction is closely related to the mesh generated in the computational domain. Hence, a set of mesh sizes (coarse to fine) is assigned to the domain specifically on the turbine surface and rotating domain. The analysis is said to converge when further reducing the mesh size does not give a significant effect to the results, i.e. turbine torque, power coefficient. Longer computational time is required for a fine mesh even though it can contribute to increasing the prediction accuracy [17]. A layer of fine mesh across the computational domain is defined to capture

the wake behind the rotating Savonius turbine. Figure 2 shows the mesh condition for the present CFD analysis.

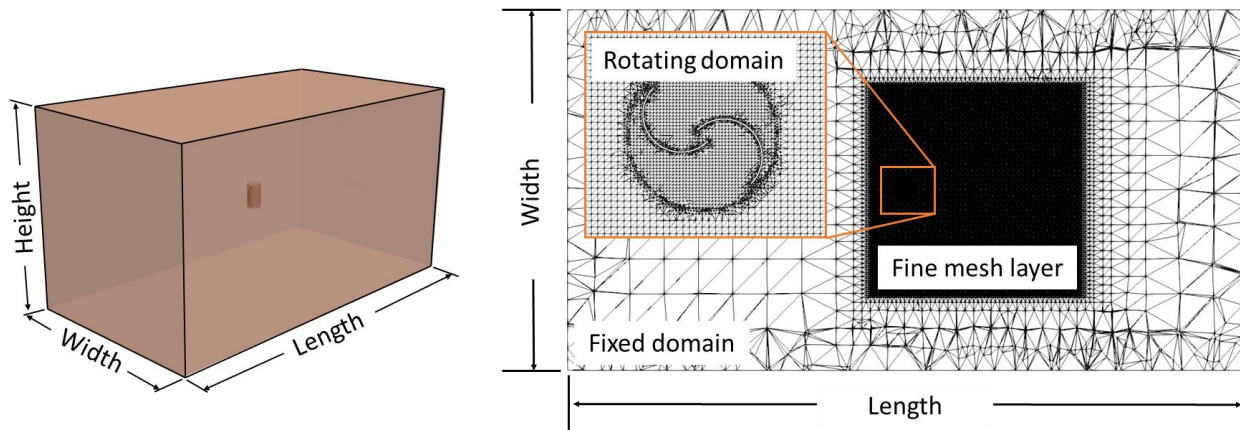


Fig. 2. 3D computation domain and mesh section view

The transient analysis was performed using finite element based solver AcuSolve incorporating the Spalart Allmaras turbulence model. The sliding mesh method used requires specific input on time step and time increment to model the turbine rotation. In this study, the turbine is allowed to rotate for 5 revolutions [18] with 10-degree movement on every time step size. The characteristics of the wake behind an isolated turbine are first evaluated by examining the formation of strong vortices for potential placement of the downstream turbine. The process for finding the best location of the downstream turbine is repeated for a different configuration. The power coefficient for each turbine is then computed by using the Eq. (2) below.

$$C_p = \frac{\tau \omega}{0.5 \rho A V^3} \quad (2)$$

where C_p is the turbine power efficiency, τ is turbine torque, ρ is the air density with a constant value of 1.225 kg/m^3 and A is turbine swept area covering the turbine diameter, D and turbine height, H .

4. Results and Discussions

4.1 Single Turbine Flow Pattern

The isolated rotating Savonius wind turbine generates a variation of flow near the turbine surface and at its downstream position and this can be represented by velocity pattern. Figure 3 shows a comparison of such patterns between a straight blade (a) and a helical blade with 90° twist angle (b). Firstly, it shows a similar pattern with the published data by CFD simulation and PIV study [11,19]. At the blade position shown, the formation of a strong vortex (I) is evident at the tip of the advancing blade for both wind turbine models. Also seen is the overlap flow [11] or overlap jet that enhances the velocity growth at the concave side of advancing blade near the blade gap direct to the concave side of returning blade, hence reduces the negative torque experienced by the turbine at certain rotor angle [20]. The low-speed zone (indicated by III) of the helical blade model appears to be smaller than the straight blade, hence the flow stream recovery is faster and increases the possibility of placement consecutive turbine near to upstream turbines. This is an advantage of the helical blade compared to the straight blade. From this analysis, it is only logical to place a downstream turbine at the location where the vortex is the strongest. At this stage, it is assumed the location is between 20° to 90° with respect to the incoming wind direction.

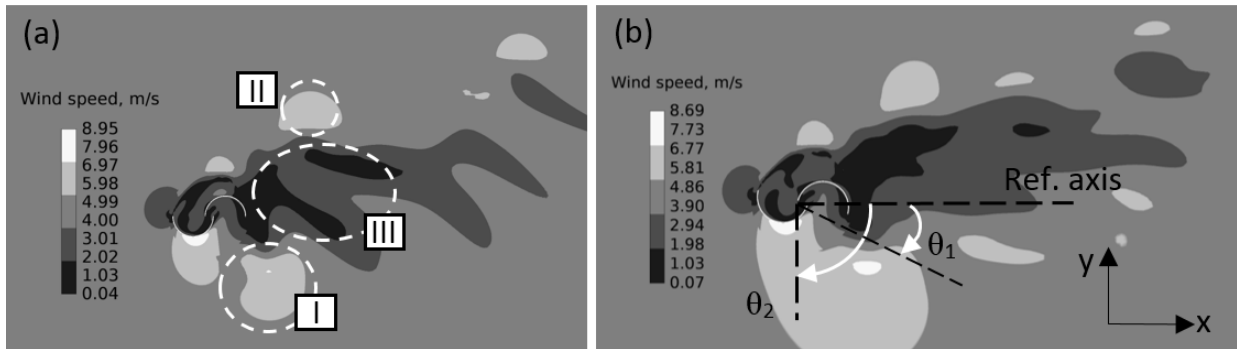


Fig. 3. Velocity pattern showing I: Periodic high-speed zone, II: Secondary periodic high-speed zone, III: Low-speed zone for a single blade CCW direction: (a) Straight blade (b) Helical blade with 90° twist

4.2 Two-turbines and Three-turbines Configuration

To understand the multiple turbine interaction further, a two-turbines and three-turbines in a line array were created based on the rule established in 4.1. The first downstream turbine is located at 60° with a gap distance of 1-Diameter [11] as shown in Figure 4. The result shows the power coefficient of turbine #2 higher than the turbine #1. This finding is a good agreement with the published data [11].

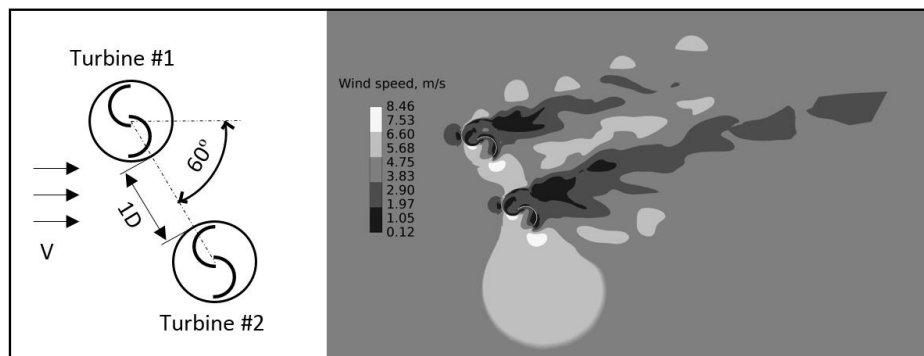


Fig. 4. Oblique two turbines configuration [11] and velocity contour generated by CFD analysis

The three-turbine array is an extended version of oblique two turbines configuration with the same gap distance and turbine relative angle as shown in Figure 5. Figure 6 shows the power enhancement of each individual turbine when compared with the isolated turbine. The individual power coefficient of turbine #2 and turbine #3 slightly improved, hence contributing to the overall turbine performance by 11%.

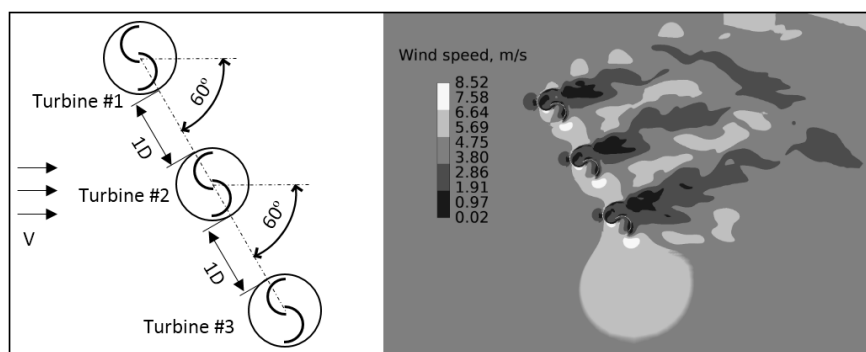


Fig. 5. Oblique three turbines configuration and velocity contour

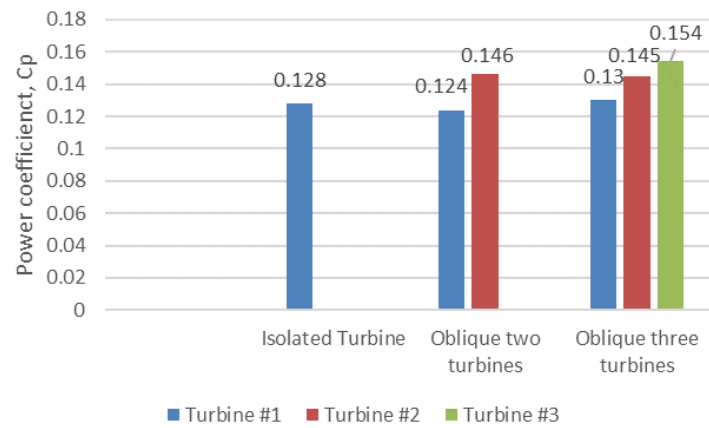


Fig. 6. Power coefficient of the individual turbine for the two-turbine and three-turbine oblique configurations

4.3 Analysis of Turbines in V-formation

Two types of turbine configuration in V-formation comprising nine turbines were examined: Case A: co-rotation and Case B: counter-rotation with a gap distance of 1-Diameter and θ of 60° . All nine turbines were designed to rotate in a counter-clockwise rotation in case A (Figure 7). Likewise, in case B, the turbines on the retuning blade side of the upstream turbine were allowed to rotate in a clockwise direction while others in the opposite direction (Figure 8).

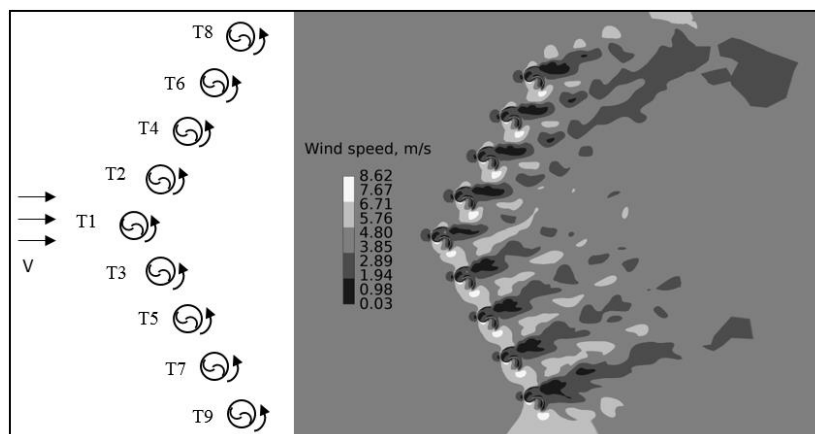


Fig. 7. Case A: Turbines in CCW direction and their velocity pattern

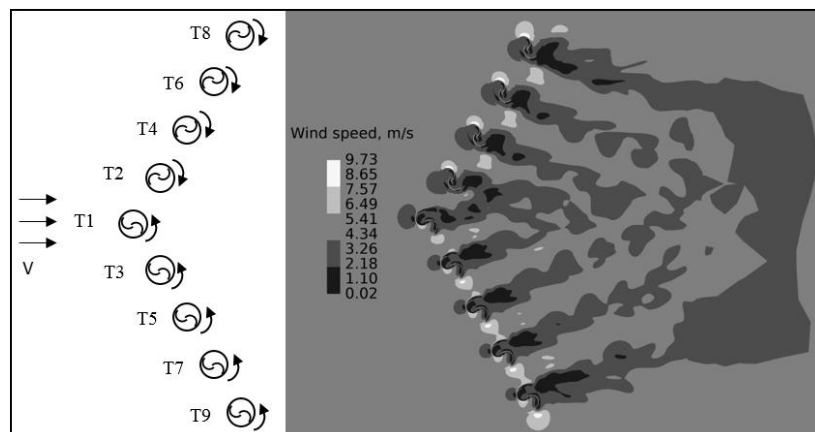


Fig. 8. Case B: A mixed of CCW and CW turbine configuration and their velocity pattern

The results of power coefficients for individual turbines are presented in Figure 9. The turbine arranged in co-rotation shows enhancement of overall power coefficient up to 9%. However, in the case of counter-rotation, an improvement of 11% of power efficiency was achieved. The highest power coefficient generated is from Turbine 8 and Turbine 9 of the V formation in Case B with power enhancement of 20% and 26% respectively. This finding is however slightly different from the published data [9], in which the power coefficient for the optimized layout of the last three downstream turbines in the array is seemed to be constant after a rapid rise in the second turbine but the overall power enhancement is 23%.

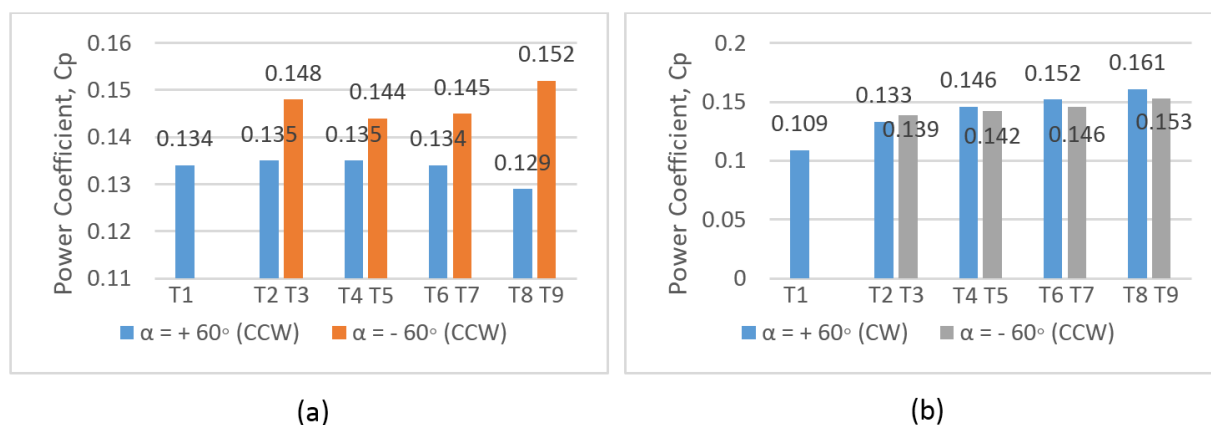


Fig. 9. Power Coefficients for V configuration in (a) co-rotation and (b) counter-rotation

5. Conclusions

In the case of a Savonius rotor, the wake generated by its rotation has created vortices that can clearly be identified by the velocity pattern. This is achieved by the zone mesh adaption strategy adopted in this analysis. Hence placing a turbine within this location will certainly improve its power efficiency. A properly arranged Savonius rotors in V formation increases the overall power efficiency of up to 11% when evaluated at 5 m/s wind speed. The performances for the co-rotation and counter-rotation of this configuration are almost the same.

Although the zone mesh adaption is an effective strategy if one is to observe the wake and vortices generated by the Savonius rotor, other turbulence simulation models may be used to improve visualization of velocity patterns. Current work is being undertaken to investigate other turbines configuration by using the detached eddy simulation (DES) model and validation by wind tunnel test.

Acknowledgment

The authors would like to acknowledge the Malaysian Electricity Supply Industries Trust Account (MESITA) through the Ministry of Energy, Science, Technology, Environment & Climate Change (MESTECC) for funding this research.

References

- [1] Dosaev, Marat Z., Lyubov A. Klimina, Boris Ya Lokshin, Yuri D. Selyutskiy, and Shih-Shin Hwang. "On Optimization of Power Coefficient of HAWT." *Journal of Power and Energy Engineering* 2, no. 4 (2014): 198-202. <https://doi.org/10.4236/jpee.2014.24028>
- [2] Khaled, Mohamed, Mostafa Mohamed Ibrahim, Hesham ElSayed Abdel Hamed, and Ahmed Farouk Abdel Gawad. "Aerodynamic design and blade angle analysis of a small horizontal-axis wind turbine." *American Journal of Modern Energy* 3, no. 2 (2017): 23-37. <https://doi.org/10.11648/j.ajme.20170302.12>

- [3] Sagharichi, Amir, Moammad Javad Maghrebi, and Alireza ArabGolarcheh. "Variable pitch blades: An approach for improving performance of Darrieus wind turbine." *Journal of Renewable and Sustainable Energy* 8, no. 5 (2016): 053305.
<https://doi.org/10.1063/1.4964310>
- [4] Rezaeiha, Abdolrahim, Ivo Kalkman, and Bert Blocken. "Effect of pitch angle on power performance and aerodynamics of a vertical axis wind turbine." *Applied energy* 197 (2017): 132-150.
<https://doi.org/10.1016/j.apenergy.2017.03.128>
- [5] Alom, Nur, and Ujjwal K. Saha. "Four decades of research into the augmentation techniques of Savonius wind turbine rotor." *Journal of Energy Resources Technology* 140, no. 5 (2018): 050801.
<https://doi.org/10.1115/1.4038785>
- [6] Tjahjana, Dominicus Danardono Dwi Prija, Syamsul Hadi, Yoga Arob Wicaksono, Diniar Mungil, Fahrudin Kurniawati, Ilham Satrio Utomo, and Sukmaji Indro Cahyono and Ari Prasetyo. "Study on Performance Improvement of the Savonius Wind Turbine for Urban Power System with Omni-directional Guide Vane (ODGV)." *Journal of Advanced Research in Fluid Mechanics and Thermal Sciences* 55, no. 1 (2019): 126-135.
- [7] Whittlesey, Robert W., Sebastian Liska, and John O. Dabiri. "Fish schooling as a basis for vertical axis wind turbine farm design." *Bioinspiration & biomimetics* 5, no. 3 (2010): 035005.
<https://doi.org/10.1088/1748-3182/5/3/035005>
- [8] Shigetomi, Akinari, Yuichi Murai, Yuji Tasaka, and Yasushi Takeda. "Interactive flow field around two Savonius turbines." *Renewable energy* 36, no. 2 (2011): 536-545.
<https://doi.org/10.1016/j.renene.2010.06.036>
- [9] Zhang, Baoshou, Baowei Song, Zhaoyong Mao, and Wenlong Tian. "A novel wake energy reuse method to optimize the layout for Savonius-type vertical axis wind turbines." *Energy* 121 (2017): 341-355.
<https://doi.org/10.1016/j.energy.2017.01.004>
- [10] Belkacem, Belabes, and Marius Paraschivoiu. "CFD Analysis of a Finite Linear Array of Savonius Wind Turbines." In *Journal of Physics: Conference Series*, vol. 753, no. 10, p. 102008. IOP Publishing, 2016.
<https://doi.org/10.1088/1742-6596/753/10/102008>
- [11] Shaheen, Mohammed, Mohamed El-Sayed, and Shaaban Abdallah. "Numerical study of two-bucket Savonius wind turbine cluster." *Journal of Wind Engineering and Industrial Aerodynamics* 137 (2015): 78-89.
<https://doi.org/10.1016/j.jweia.2014.12.002>
- [12] Kirchner-Bossi, Nicolas, and Fernando Porté-Agel. "Realistic Wind Farm Layout Optimization through Genetic Algorithms Using a Gaussian Wake Model." *Energies* 11, no. 12 (2018): 3268.
<https://doi.org/10.3390/en1123268>
- [13] Sun, Xiaojing, Daihai Luo, Dianguai Huang, and Guoqing Wu. "Numerical study on coupling effects among multiple Savonius turbines." *Journal of Renewable and Sustainable Energy* 4, no. 5 (2012): 053107.
<https://doi.org/10.1063/1.4754438>
- [14] Shaheen, Mohammed, and Shaaban Abdallah. "Development of efficient vertical axis wind turbine clustered farms." *Renewable and Sustainable Energy Reviews* 63 (2016): 237-244.
<https://doi.org/10.1016/j.rser.2016.05.062>
- [15] Zakaria, Ahmad and M.S.N. Ibrahim. "Numerical performance evaluation of savonius rotors by flow-driven and sliding-mesh approaches." *International Journal of Advanced Trends in Computer Science and Engineering* 8, no. 1 (2019): 57-61.
<https://doi.org/10.30534/ijatcse/2019/10812019>
- [16] Tian, Wenlong, Baowei Song, James H. VanZwieten, and Parakram Pyakurel. "Computational fluid dynamics prediction of a modified Savonius wind turbine with novel blade shapes." *Energies* 8, no. 8 (2015): 7915-7929.
<https://doi.org/10.3390/en8087915>
- [17] Ghasemian, Masoud, Z. Najafian Ashrafi, and Ahmad Sedaghat. "A review on computational fluid dynamic simulation techniques for Darrieus vertical axis wind turbines." *Energy Conversion and Management* 149 (2017): 87-100.
<https://doi.org/10.1016/j.enconman.2017.07.016>
- [18] Kumar, Anuj, and R. P. Saini. "Performance analysis of a single stage modified Savonius hydrokinetic turbine having twisted blades." *Renewable Energy* 113 (2017): 461-478.
<https://doi.org/10.1016/j.renene.2017.06.020>
- [19] Dobrev, Ivan, and Fawaz Massouh. "Exploring the flow around a Savonius wind turbine." In *Proceedings of the 16th International Symposium on Applications of Laser Techniques to Fluid Mechanics Lisbon, Portugal*. 2012.
- [20] Kacprzak, Konrad, Grzegorz Liskiewicz, and Krzysztof Sobczak. "Numerical investigation of conventional and modified Savonius wind turbines." *Renewable Energy* 60 (2013): 578-585.
<https://doi.org/10.1016/j.renene.2013.06.009>